Existence and Stability of Spherically Layered Solutions of the Diblock Copolymer Equation

Xiaofeng Ren *
Department of Mathematics and Statistics
Utah State University
Logan, UT 84322-3900, USA

Juncheng Wei †
Department of Mathematics
Chinese University of Hong Kong
Shatin, Hong Kong

November 10, 2004

Abstract

The relatively simple Ohta-Kawasaki density functional theory for diblock copolymer melts may be analytically studied in many situations by singular perturbation techniques. We consider a single sphere pattern that constitutes a cell in the important spherical phase of a diblock copolymer. We show the existence of the sphere pattern as a solution of the Euler-Lagrange equation of the free energy. Quantitative properties of the solution are derived, from which we determine the optimal size of the sphere. Moreover there is a stability threshold so that if the sphere is larger than the threshold value, the sphere pattern is no longer stable. The same issues are discussed for a spherical lamellar pattern, which may be viewed as a defective lamellar phase. Here we reduce the existence and the stability problems to some finite dimensional problems. Quantitative information on the solution of the original infinite dimensional problem is obtained.

Keywords: Ohta-Kawasaki diblock copolymer theory, sphere pattern, spherical lamellar pattern, existence threshold, stability threshold.

1 Introduction

A diblock copolymer melt is a soft material, characterized by fluid-like disorder on the molecular scale and a high degree of order at a longer length scale. A molecule in a diblock copolymer is a linear sub-chain of A-monomers grafted covalently to another sub-chain of B-monomers. Because of the repulsion between the unlike monomers, the different type sub-chains tend to segregate, but as they are chemically bonded in chain molecules, segregation of sub-chains cannot lead to a macroscopic phase separation. Only a local micro-phase separation occurs: micro-domains rich in A and B emerge as a result. These micro-domains form morphology patterns/phases.

There are two types of phase separations in a diblock copolymer system: weak segregation and strong segregation. The weak segregation occurs when the temperature is relatively high. The micro-domains are small and the there are no clear interfaces separating them. When the temperature is

*Corresponding author. Phone: 1 435 797-0755, Fax 1 435 797-1822, E-mail: ren@math.usu.edu
†Supported in part by a Direct Grant from CUHK and an Earmarked Grant of RGC of Hong Kong.

lower, strong segregation is observed. The micro-domains become larger and they are separated by narrow interfaces.

The self-consistent mean field theory [10, 12, 13, 14, 16, 17] is the most successful theory in modeling and capturing aspects of the phase separation. It consists of five equations for five field variables: two density fields of A- and B-monomers, two mean fields on A- and B-monomers simulating the interaction between the molecular chains, and a Lagrange multiplier field. Two of the five equations are nonlocal, while the remaining three are algebraic [21]. The theory is derived from a microscopic description of interacting polymer chains. Based on a variational principle, the Gibbs canonical distribution is approximated by the distribution generated by the mean fields [6]. This theory is quite complex to which only numerical studies have been done. One of them is the spectral method of Matsen and Schick [21] that yields predictions with striking resemblances to experiments.

A limitation of such techniques or other test field based methods is that they proceed by assuming a periodic structure, computing its free energy and then comparing that free energy to the free energy of other candidate structures [3]. The patterns found by such methods in general do not exactly solve the self-consistent equations. However finding analytic solutions to these equations is very difficult due to the complexity of the two integral equations.

The density functional theory of Ohta and Kawasaki [26] is a much simpler model. The free energy of a diblock copolymer melt is an elegant functional of the A-monomer density field only (2.2). Unlike an earlier density functional theory of Leibler [19] that only deals with the weak segregation region, the Ohta-Kawasaki theory deals with both the weak- and strong-segregation phenomena. The Euler-Lagrange equation of the Ohta-Kawasaki free energy is an integro-differential equation (2.9), which can also be viewed as a system of two elliptic partial differential equations (2.11-2.12).

A close examination of the derivation of the theory [6] shows that it is a simplified version of the self-consistent mean field theory. Two approximation steps are used. First the dependence of the monomer density fields on the mean fields is linearized. The approximation is less accurate if the temperature is too low. Then this linear dependence is reversed so that the mean fields depend linearly on the density fields. The second approximation is used here so that only the long wave and the short wave effects of this dependence (in the Fourier space) are retained. Intermediate wave effects are ignored.

Despite the shortcomings associated with these approximations, the density functional theory at least qualitatively captures the properties of diblock copolymers [20, 9]. Although Ohta and Kawasaki only applied their theory to test fields and did not construct exact solutions of the Euler-Lagrange equation, we will show that the simplicity of the theory actually makes it possible to study exact solutions analytically.

The weak segregation regime may be studied by the bifurcation theory rather easily. One starts with a uniform state and linearizes the Euler-Lagrange equation at the uniform state. For some parameter values the principal eigenvalue of the linearized problem is zero. Then a non-uniform state bifurcates from the uniform state. If one can show that this non-uniform state is stable, then it gives the profile of a weakly segregated pattern.

In this paper we use the density functional theory to study the more complex strong segregation phenomenon. Strongly segregated patterns are too different from the uniform state to be treated as bifurcation solutions. The appropriate mathematical theory is the singular perturbation theory in calculus of variations and differential equations. It allows one to go beyond the test field argument and find exact solutions, or at least leading order terms of exact solutions, to the Euler-Lagrange equation of the free energy functional [25, 28, 30, 29, 33, 38, 37, 8, 5, 15]. Often these solutions may be carefully analyzed and their stability in space can be determined [31, 36].

Figure 1: The spherical phase. The dark color indicates the concentration of B-monomers, and the white color indicates A-monomers. Not reflected in this figure is the body centered cubic pattern in which the spheres pack.

The first strongly segregated pattern we study is the single sphere pattern. This pattern arises from the spherical phase of a diblock copolymer. When the monomer fraction is skewed in favor of A-monomers, the B-monomers form spherical micro-domains, Figure 2. For a wide range of sphere size we will find a solution to the Euler-Lagrange equation whose shape matches that of a sphere. After we find the free energy of the solution, we discover that there is an optimal size for the sphere. The sphere of the optimal size has lower free energy than that of any other sphere. Then we linearize the Euler-Lagrange equation at the sphere solution and study the spectrum of the linearized operator. We will show that there is an upper bound for the size of the sphere. Beyond the upper bound, the sphere can not be stable.

The second pattern is the spherical lamellar pattern. This pattern may be viewed as a defective lamellar pattern. Other defective patterns are considered in [41] where a model of a forth order differential equation is used. Given the number of interfaces we look for a solution that consists of spherical layers of micro-domains separated by narrow interfaces. In this case the existence and stability problems are drastically reduced to some finite dimensional problems. The reduced problems are easily solved by computer. Note that here we apply numerical studies to the reduced finite dimensional problems. They yield far more accurate results compared to direct numerical studies of the infinite dimensional problems. One obtains quantitative information on the solution. We again determine the stability threshold. Moreover we find an existence threshold.

We emphasize that all the results presented in this paper are mathematically rigorous. The informal style adopted here when we describe perturbation expansions can be changed to a strict mathematical framework, part of which is known as the Γ-convergence theory [7, 23, 22, 18].

2 Free energy

The density functional theory of Ohta and Kawasaki views the free energy of a diblock copolymer melt as a functional of the relative A-monomer density field $u(x)$ where x is a point in a sample D. The melt is assumed to be incompressible, so the number density of the combined A- and B-monomers is uniform in space. $u(x)$ is the A-monomer number density at x divided by the combined A- and B-monomer number density. When $u(x) = 1$ (or $u(x) = 0$, respectively), the point x is occupied by A-monomers (or B-monomers, respectively); if $0 < u(x) < 1$, a mixture of A- and B-monomers occupies x. Let N_A be the number of the A-monomers in a chain molecule and N_B be the number of the B-monomers. $N = N_A + N_B$ is the polymerization index. u must satisfy the constraint

$$\overline{u} = a \tag{2.1}$$

where $\overline{u} = \frac{1}{|D|}\int_D u(x)\,dx$ is the average of u, and $a = N_A/N$ is the A-monomer fraction in a chain molecule.

In a dimensionless form the free energy is written as

$$\int_D [\frac{\epsilon^2}{2}|\nabla u|^2 + W(u) + \frac{\epsilon\gamma}{2}|(-\Delta)^{-1/2}(u-a)|^2]\,dx. \tag{2.2}$$

The physical parameters of the diblock copolymer system include

1. The polymerization index N that is the number of all the monomers in a chain molecule. We consider the ideal situation where this N is the same in all molecules;
2. The A-monomer number N_A and the B-monomer number N_B in a chain. Again N_A and N_B are the same in all molecules;
3. The Kuhn statistical length l measuring the average distance between two adjacent monomers in a chain molecule, which is the same regardless the monomer types;
4. The dimensionless Flory-Huggins parameter χ that measures the repulsion between unlike monomers;
5. The volume V of the sample.

The Flory-Huggins parameter χ is defined by

$$\chi = \beta(V_{AB} - \frac{V_{AA} + V_{BB}}{2}) \tag{2.3}$$

where V_{AB} (and V_{AA}, V_{BB} respectively) is the energy cost to bring an A-monomer (A-monomer and B-monomer respectively) and a B monomer (A-monomer and B-monomer respectively) close to each other. This number is positive because the repulsion force between unlike monomers is stronger than those between like ones. β is the inverse temperature, and henceχ is inversely proportional to temperature.

In [6] the three dimensionless parameters ϵ, γ and a in (2.2) are related to the physical parameters via

$$\epsilon^2 = \frac{|D|^{2/3}l^2}{12a(1-a)\chi V^{2/3}}, \tag{2.4}$$

$$\gamma = \frac{18\sqrt{3}V}{|D|a^{3/2}(1-a)^{3/2}\chi^{1/2}N^2l^3}. \tag{2.5}$$

The sample domain D in (2.2) has already been re-scaled. In (2.4) and (2.5) $|D|$ is the volume of D after re-scaling. One could take it to be 1, but in this paper D will be a ball, so it is more convenient to have the the radius of D to be 1 and $|D| = 4\pi/3$.

The re-scaled free energy (2.2) is

$$(2.2) = \frac{\beta F}{\chi \rho_0 V} \tag{2.6}$$

where F is the free energy and ρ_0 the average number of monomers per volume [6]. If n is the number of the molecular chains in the melt, then $\rho_0 = \frac{nN}{V}$. Hence (2.2) is the free energy per monomer multiplied by β/χ.

The exact form of W is not given in [26]. In [6] an approximation

$$W(u) = \begin{cases} u - u^2 & \text{if } u \in [0,1] \\ \infty & \text{otherwise} \end{cases} \tag{2.7}$$

is found. A more accurate W should be a smooth double well function of equal depth. It must have a global minimum value 0 achieved at 0 and 1. It must have the symmetry $W(u) = W(1-u)$. 0 and 1 are non-degenerate: $W''(0) = W''(1) > 0$.

Central in (2.2) is the third term in the integrand. It is nonlocal and models the long range interaction between monomers due to the connectivity of the molecular chains. The operator $(-\Delta)^{-1}$ is the square root of the inverse of $-\Delta$ with the natural boundary condition. Alternatively one may write

$$\int_D |(-\Delta)^{-1/2}(u-a)|^2 \, dx = \int_D \int_D (u(x)-a)G(x,y)(u(y)-a) \, dxdy \tag{2.8}$$

where G is the Green function of $-\Delta$ with the natural boundary condition.

The second term in (2.2) can be regarded as the internal energy field of the system, and the first and the third terms give the entropy of the system. As mentioned in the introduction we have only taken the long wave and short wave effects, modeled by the ∇ and $(-\Delta)^{-1/2}$ operators, into consideration.

The first term in the integrand of (2.2) penalizes any space non-uniformity. The second term prefers u being either close to 0 or close to 1 everywhere. The best profile for the third term is to have u close to a everywhere. However this is not a good profile for the second term. The second best profile for the third term is for u to have many oscillations. Local minimizers of the free energy result from the three competing effects.

The Euler-Lagrange equation of (2.2) is a nonlinear integro-differential equation:

$$-\epsilon^2 \Delta u + f(u) + \epsilon\gamma(-\Delta)^{-1}(u-a) = \eta \text{ in } D \tag{2.9}$$

subject to the natural boundary condition

$$\partial_\nu u = 0 \text{ on } \partial D. \tag{2.10}$$

Here $f = W'$. The constant η on the right side of (2.9) is a Lagrange multiplier because of the constraint (2.1). The equation (2.9) may also be written as a system of elliptic partial differential equations:

$$-\epsilon^2 \Delta u + f(u) + \epsilon\gamma v = \eta \tag{2.11}$$

$$-\Delta v = u - a \tag{2.12}$$

subject to the conditions

$$\partial_\nu u = \partial_\nu v = 0 \text{ on } \partial D, \ \overline{u} - a = \overline{v} = 0. \tag{2.13}$$

Note that (2.9) always has the uniform solution $u(x) = a$. When ϵ is large, corresponding to high temperature, this solution is stable and it models the disordered phase. One may decrease ϵ to a value so that the principal eigenvalue of the linearized problem at $u(x) = a$ becomes 0. Then one finds a non-uniform solution bifurcating out of the uniform solution. This bifurcation solution gives the profile in the weak segregation regime and the corresponding ϵ identifies the parameter range for weak segregation.

However in the strong segregation regime ϵ is much smaller. In this case the free energy (2.2) is mostly easily analyzed in the parameter range

$$\epsilon \ll 1 \tag{2.14}$$

$$\gamma \sim 1. \tag{2.15}$$

Here the uniform solution $u(x) = a$ has much higher free energy than those of many other states and is hence thermodynamically un-favored. Under (2.14-2.15), we are in the strong segregation regime and have taken the size of the sample to be of order

$$V \sim a^{3/2}(1-a)^{3/2}\chi^{1/2}N^2l^3. \tag{2.16}$$

We will see that in the parameter range (2.14-2.15) the number of micro-domains is of order 1. Therefore the right side of (2.16) also predicts the size of a micro-domain.

Having a small ϵ makes (2.9) a singular perturbation problem. Although the singular perturbation theory is much harder and less mature than the regular perturbation theory, a great deal of quantitative properties of solutions to (2.9) can be obtained, using the existing theoretical techniques in the theory. Some problems are solved exactly in the leading order, and some other problems are reduced to much simpler finite dimensional problems and are accurately solved with the help of computer.

3 Sphere pattern

When the monomer fraction a is close to 1, the diblock polymer typically exists in the spherical phase. B-rich micro-domains form spheres and pack in a body centered cubic pattern. Here we study a single sphere based on the model (2.2).

3.1 Existence

When one takes the domain D to be a unit ball, a radially symmetric solution $u(r)$ of (2.9) is found where u now is a function of $r = |x|$, Figure 2. A narrow interface, whose thickness is of order ϵ, exists at some r_1 where $u(r_1) = 1/2$. The leading order of r_1 is determined by (2.1):

$$r_1 = (1-a)^{1/3} + O(\epsilon). \tag{3.17}$$

Inside the interface $u(r)$ is close to 0 and outside $u(r)$ is close to 1. The profile of u near r_1 is described by $H(\frac{r-r_1}{\epsilon})$ where H is a function that solves

$$-H'' + f(H) = 0 \tag{3.18}$$

Figure 2: A single sphere solution with the natural boundary condition in the unit ball.

with the conditions $H(-\infty) = 0$, $H(\infty) = 1$, and $H(0) = 1/2$.

With more effort we find the next term in the inner asymptotic expansion of u. Denote this term by P so that

$$u(r) = H(\frac{r - r_1}{\epsilon}) + \epsilon P(\frac{r - r_1}{\epsilon}) + O(\epsilon^2). \tag{3.19}$$

P is the solution of

$$-P'' + f'(H)P - \frac{2H'}{r_1} + \frac{2\tau}{r_1} = 0, \ P(0) = 0. \tag{3.20}$$

The definition of P involves r_1. Because $1/r_1$ is the mean curvature of the interface, we see that the curvature affects the inner expansion of u in the ϵ order but not in the leading order, for H is independent of r_1.

In (3.20) we have introduced a constant τ, which is known as the interface tension. For a general W,

$$\tau = \int_0^1 \sqrt{2W(s)}dx, \tag{3.21}$$

and for (2.7) we have

$$\tau = \frac{\sqrt{2}\pi}{8}. \tag{3.22}$$

This value of τ differs from the one obtained in [11] by a mean field theory.

The free energy of this solution may be viewed as a sum of two parts. The first part comes from the two local terms of (2.2) and is equal to

$$4\pi r_1^2 \tau\epsilon + O(\epsilon^2). \tag{3.23}$$

Note that the first term on the right side is the area of the interface times τ times ϵ.

The second part of the free energy comes from the nonlocal term of (2.2) and is equal to

$$\frac{2\pi r_1^5 (r_1^3 - 3r_1 + 2)\gamma\epsilon}{15} + O(\epsilon^2). \tag{3.24}$$

a	.5	.525	.55	.575	.6	.625	.65	.675	.7	.725
γ_o	140	130	122	115	109	104	100	97	95	93

a	.75	.775	.8	.825	.85	.875	.9	.925	.95	.975
γ_o	92	92	93	95	99	106	117	137	176	290

Table 1: The values of γ_o for various a.

Note that the free energy of the disordered phase modeled by the uniform solution $u(x) = a$ is $W(a)|D|$, a quantity of order 1, which is much larger than the free energy of the sphere pattern solution which is of order ϵ. We are assured that (2.14-2.15) give an ordered phase.

3.2 Optimal size

There is a sphere pattern solution of (2.9) for any γ as long as ϵ is sufficiently small. This means that there is a solution for a wide range of V of the sample (the volume of the B-monomer sphere in the middle is then $(1-a)V$). It is natural to ask for which value of V the sphere pattern is mostly energetically favored. Intuitively we know that V can not be too large or too small. By (2.4-2.5) we write $\epsilon = \tilde{\epsilon} V^{-1/3}$ and $\gamma = \tilde{\gamma} V$ so that $\tilde{\epsilon}$ and $\tilde{\gamma}$ no longer depend on V. Then by (3.23-3.24) we find that the leading term of the re-scaled free energy of a sphere pattern is

$$4\pi r_1^2 \tau \tilde{\epsilon} V^{-1/3} + \frac{2\pi r_1^5 (r_1^3 - 3r_1 + 2)\tilde{\gamma}}{15} \tilde{\epsilon} V^{2/3}. \tag{3.25}$$

With respect to V, (3.25) is minimized at

$$V = V_o = \frac{15\tau}{r_1^3 (r_1^3 - 3r_1 + 2)\tilde{\gamma}}. \tag{3.26}$$

The optimal size of the sample is now given by (3.26). It is more convenient to express this in terms of the dimensionless γ. The optimal γ is denoted by γ_o which is just

$$\gamma_o = \tilde{\gamma} V_o = \frac{15\tau}{r_1^3 (r_1^3 - 3r_1 + 2)}. \tag{3.27}$$

Table 1 reports the values of γ_o for various a.

3.3 Stability

We return to a sphere pattern solution with a general γ which is not necessarily equal to γ_o. Although a sphere solution of (2.9) is found for any γ, we will see that it is stable only if γ is not too large. A stable solution of (2.9) is a free energy local minimizer, which corresponds to a meta-stable state of the physical system. An unstable solution can not be observed in experiments.

The stability analysis requires that we solve the eigenvalue problem

$$-\epsilon^2 \Delta \varphi + f'(u)\varphi - \overline{f'(u)\varphi} + \epsilon\gamma(-\Delta)^{-1}\varphi = \lambda\varphi. \tag{3.28}$$

The left side of (3.28) comes from linearizing the Euler-Lagrange equation (2.9) at a sphere pattern solution u. The eigenvalues λ are classified into λ_l where $l = 0, 1, 2, ...$ is the mode. The eigenfunctions take the form

$$\varphi(x) = \phi_l(r) Y_{lm}(\theta, \omega) \tag{3.29}$$

where $m = 0, \pm 1, ..., \pm l$, and the Y_{lm}'s are the spherical harmonics. An eigenvalue either approaches 0, a critical eigenvalue, or stays positively away from 0 when $\epsilon \to 0$. Hence we will only consider the critical eigenvalues.

For the $l = 0$ mode there is one critical eigenvalue of order ϵ. It is of multiplicity 1 and has the form

$$\lambda_0 = \frac{3f'(0)r_1^2\epsilon}{\tau} + O(\epsilon^2). \tag{3.30}$$

This eigenvalue is positive, and $l = 0$ is a stable mode. The eigenfunction associated with this eigenvalue is radially symmetric. We write it as $\phi_0(r)$. It has the expansion

$$\phi_0(r) = H'(\frac{r - r_1}{\epsilon}) + \epsilon P'(\frac{r - r_1}{\epsilon}) - \overline{[H'(\frac{r - r_1}{\epsilon}) + \epsilon P'(\frac{r - r_1}{\epsilon})]} + O(\epsilon^2). \tag{3.31}$$

Here H' and P' are the derivatives of H and P, defined in (3.18-3.19), respectively.

For $l = 1$ there is one critical eigenvalue of order ϵ^2. It is of multiplicity 3 and has the form

$$\lambda_1 = \frac{\gamma r_1^4 \epsilon^2}{\tau} + O(\epsilon^3). \tag{3.32}$$

This mode is again stable. The eigenfunctions associated with this eigenvalue are $(x/r)\phi_1(r)$, $(y/r)\phi_1(r)$, and $(z/r)\phi_1(r)$ where ϕ_1 has the expansion

$$\phi_1(r) = H'(\frac{r - r_1}{\epsilon}) + \epsilon P'(\frac{r - r_1}{\epsilon}) + O(\epsilon^2). \tag{3.33}$$

For each l greater than 1, there is one critical eigenvalue of order ϵ^2. It is of multiplicity $2l + 1$ and has the form

$$\lambda_l = [\frac{l(l+1) - 2}{r_1^2} + \frac{\gamma}{\tau}(\frac{r_1^4 - r_1}{3} + \frac{(l+1)r_1^{2l+2}}{l(2l+1)} + \frac{r_1}{2l+1})]\epsilon^2 + O(\epsilon^3). \tag{3.34}$$

The quantity in (3.34) may not always be positive. One finds a threshold γ_s so that when $\gamma < \gamma_s$ all the eigenvalues in (3.34) are positive, but when $\gamma > \gamma_s$ at least for one l the eigenvalue λ_l in (3.34) is negative. Therefore the sphere solution u is stable if $\gamma < \gamma_s$ and unstable if $\gamma > \gamma_s$. The eigenfunctions associated with λ_l are $\phi_l(r)Y_{lm}$ with $m = 0, \pm 1, ..., \pm l$. ϕ_l has the same expansion as in (3.33).

The leading order of γ_s is determined from (3.34) following these steps:

1. For each $l \geq 2$, set the leading term

$$\frac{l(l+1) - 2}{r_1^2} + \frac{\gamma}{\tau}(\frac{r_1^4 - r_1}{3} + \frac{(l+1)r_1^{2l+2}}{l(2l+1)} + \frac{r_1}{2l+1}) \tag{3.35}$$

in (3.34) to be 0, and solve for γ. Denote the solution for γ by $\hat{\gamma}_l$. If this $\hat{\gamma}_l$ is less than or equal to 0, the mode l does not yield a zero eigenvalue. Discard such $\hat{\gamma}_l$.

a	.5	.525	.55	.575	.6	.625	.65	.675	.7	.725
γ_s	463	425	372	336	312	296	276	250	234	225
l	5	5	4	4	4	4	3	3	3	3

a	.75	.775	.8	.825	.85	.875	.9	.925	.95	.975
γ_s	222	225	232	216	209	215	237	283	387	714
l	3	3	3	2	2	2	2	2	2	2

Table 2: The (leading order) values of γ_s for various a and the corresponding mode l.

Figure 3: A perfect lamellar pattern.

2. Minimize the remaining $\hat{\gamma}_l$'s from the last step with respect to l. The minimum is achieved at a $\hat{\gamma}_l$ which is the leading order of γ_s.

Table 2 reports γ_s for various a. At $\gamma = \gamma_s$ the smallest eigenvalue is 0. The mode l of this eigenvalue is also given in Table 2.

We compare the stability threshold γ_s to the optimal size γ_o in Table 1. All the γ_o's are significantly less than the corresponding γ_s's. Hence, not surprisingly, the optimal size is in the stable region.

4 Spherical lamellar pattern

When a is close to $1/2$, the diblock copolymer exists in the lamellar phase. The perfect lamellar pattern consists micro-domains separated by parallel flat planes, Figure 3. However one often observes the lamellar pattern in defective forms. The spherical lamellar pattern, Figure 4, is one of them.

Because it involves many interfaces, the study in this section is more complex. Nevertheless we will show that by singular perturbation argument, solving the Euler-Lagrange equation (2.9) and

Figure 4: A cross section of a spherical lamellar pattern with two interfaces.

analyzing the stability of the solution are reduced to studying some finite dimensional problems. These reduced finite dimensional problems can be easily and accurately solved by computer.

4.1 Existence

Unlike the existence problem for the sphere pattern where no condition on γ is needed, the existence of a spherical lamellar pattern as a solution of (2.9) requires that γ is not too small. We now have an existence threshold $\gamma_{K,e}$. Given the number of interfaces $K \geq 2$ a K-interface spherical lamellar pattern solution of (2.9) exists if $\gamma > \gamma_{K,e}$. If $\gamma < \gamma_{K,e}$ no K-interface spherical lamellar solution can exist.

When $\gamma > \gamma_{K,e}$ and a K-interface solution u exists, we define the interfaces r_j, $j = 1, 2, ..., K$, to be such that $u(r_j) = 1/2$. They have the expansion

$$r_j = r_j^0 + O(\epsilon). \tag{4.36}$$

The leading order r_j^0's are determined by solving a system of $K+1$ nonlinear equations

$$\begin{aligned} \frac{\tau}{r_j^0} + \frac{(-1)^j \gamma}{2} \mathcal{V}(r_j^0; r_1^0, r_2^0, ..., r_K^0) &= (-1)^j \eta^0, \quad j = 1, 2, ..., K \\ \sum_{j=1}^{K} (-1)^j (r_j^0)^3 + \frac{1 - (-1)^K}{2} &= a \end{aligned} \tag{4.37}$$

for r_1^0, r_2^0,...,r_K^0, and η^0. Here η^0 is a Lagrange multiplier. The quantity $\mathcal{V}$ in (4.37) is defined as follows. Given r_1^0, r_2^0,...,r_K^0, one solves the equation

$$-\mathcal{V}'' - \frac{2}{r}\mathcal{V} = \mathcal{U} - a, \ \mathcal{V}'(0) = \mathcal{V}'(1) = 0, \ \overline{\mathcal{V}} = 0, \tag{4.38}$$

where

$$\mathcal{U}(r) = 0, \text{ if } r \in (0, r_1^0), \ = 1 \text{ if } r \in (r_1^0, r_2^0), \ .... \tag{4.39}$$

a	.5	.525	.55	.575	.6	.625	.65	.675	.7	.725
$\gamma_{2,e}$	171	175	180	186	194	204	216	230	249	271

a	.75	.775	.8	.825	.85	.875	.9	.925	.95	.975
$\gamma_{2,e}$	300	337	386	453	549	694	932	1379	2432	6590

Table 3: The leading order values of $\gamma_{2,e}$ for various a.

Denote this solution by $\mathcal{V}(r; r_1^0, ..., r_K^0)$ where we emphasize in its arguments that $\mathcal{V}$ depends on r_1^0,...,r_K^0. In (4.37) this $\mathcal{V}$ is evaluated at r_j^0.

We have observed that the determination of r_j, an infinite dimensional problem, is reduced to the determination of r_j^0, the leading order of r_j. The equations in (4.37-4.37) for r_j^0 form a much easier finite dimensional problem.

The system (4.37-4.37) is the Euler-Lagrange equations of the minimizer of the function

$$J(q_1, q_2, ..., q_K) = 3\tau \sum_{k=1}^{K} q_k^2 + \frac{3\gamma}{2} \int_0^1 \mathcal{V}'(r; q_1, ..., q_K)^2 r^2 dr \tag{4.40}$$

subject to the constraint

$$-q_1^2 + q_2^3 + ... + (-1)^K q_K^3 + \frac{1 - (-1)^K}{2} = a. \tag{4.41}$$

In the mathematics literature J is known as the Γ-limit of $(4\pi\epsilon/3)^{-1} I$. Note that for each K, J is a finite dimensional problem. The Γ-limit theory often reduces the study of the infinite dimensional problem I to the study of J [28, 29].

Whether J has a minimizer depends on γ. In general J has a minimizer if γ is large, and J does not have a minimizer if γ is small. The border line is exactly the leading order of $\gamma_{K,e}$. Hence the leading order of $\gamma_{K,e}$ is found by analyzing J. For $K = 2$, Table 3 reports the leading order of $\gamma_{2,e}$ for various a.

Let us consider the $K = 2$ case in more detail. We introduce y so that

$$y = q_1^3, \; y + a = q_2^3. \tag{4.42}$$

J can be viewed as a function of y only without the constraint (4.41). Take $a = 1/2$. For $\gamma = 100$, J is monotonically increasing in y, Figure 5. In this case of $\gamma < \gamma_{2,e}$, since $\gamma_{2,e} \approx 171$ from Table 3, there is no 2-interface spherical lamellar solution of (2.9). When $\gamma = 180 > \gamma_{2,e}$, J is no longer monotone, Figure 6. In this case J has a local minimum, and (2.9) has a 2-interface spherical lamellar solution. If we further increase γ to 200, the local minimum of J becomes a global minimum, Figure 7. The spherical lamellar solution continues to exist.

We now return to the general solution with K interfaces. Near each interface r_j the solution u again has a profile

$$u(r) = H(\frac{r - r_j}{\epsilon}) + \epsilon P_j(\frac{r - r_j}{\epsilon}) + O(\epsilon^2) \tag{4.43}$$

when j is odd and

$$u(r) = H(-\frac{r - r_j}{\epsilon}) + \epsilon P_j(-\frac{r - r_j}{\epsilon}) + O(\epsilon^2) \tag{4.44}$$

Figure 5: J as a function of y is increasing when $a = 1/2$ and $\gamma = 100$.

Figure 6: J as a function of y has a local minimum when $a = 1/2$ and $\gamma = 180$.

Figure 7: J as a function of y has a global minimum when $a = 1/2$ and $\gamma = 200$.

when j is even. H is the same function defined in (3.18) and P_j is define by (3.19) with r_1 replaced by r_j.

The free energy of this solution is

$$[4\pi\tau\sum_{j=1}^{K} r_j^2 + 2\pi\gamma\int_0^1 \mathcal{V}'(r)^2 r^2\, dr]\epsilon + O(\epsilon^2). \tag{4.45}$$

4.2 Stability

Similar to the sphere pattern solution, a K-interface spherical lamellar solution is stable only if γ is not too large. More precisely for any given number of interfaces K, there is a stability threshold $\gamma_{K,s}$, which is larger than the existence threshold $\gamma_{K,e}$, such that the K-interface spherical lamellar solution is stable if $\gamma_{K,e} < \gamma < \gamma_{K,s}$. The solution becomes unstable if $\gamma > \gamma_{K,s}$.

To verify these statements and determine $\gamma_{K,s}$ we again turn to the linearized problem (3.28). But this time u is the K-interface spherical lamellar solution found in Section IVA. The eigenvalues are classified into λ_l, $l = 0, 1, ...$ For each l the non-critical eigenvalues all stay positively away from 0, so one needs only to find the critical eigenvalues to determine whether u is stable.

When l is equal to 0, there exist K critical eigenvalues. One of them is of order ϵ and has the expansion

$$\lambda_0 = \frac{3f'(0)\sum_{k=1}^{K}(r_k^0)^2}{\tau}\epsilon + O(\epsilon^2), \tag{4.46}$$

which is positive. This eigenvalue is of multiplicity 1. The associated eigenfunction is

$$\phi_0(r) = \sum_{j=1}^{K}\{H'(\frac{r-r_j}{\epsilon}) + \epsilon P_j'(\frac{r-r_j}{\epsilon}) - \overline{[H'(\frac{r-r_j}{\epsilon}) + \epsilon P_j'(\frac{r-r_j}{\epsilon})]}\} + O(\epsilon^2). \tag{4.47}$$

The remaining $K-1$ $l=0$ mode critical eigenvalues are of order ϵ^2 and of multiplicity 1. Let us expand them as

$$\lambda_0 = \mu_0\epsilon^2 + O(\epsilon^3). \tag{4.48}$$

The determination of μ_0 is more complex.

First we define a K by K matrix M whose kj-entry is

$$\begin{cases} (-\frac{2\tau}{(r_k^0)^2} + \gamma(-1)^k\mathcal{V}'(r_k^0)) + \gamma G_0(r_k^0, r_k^0) & \text{if} \quad k = j \\ \gamma G_0(r_k^0, r_j^0) & \text{if} \quad k \neq j \end{cases} \tag{4.49}$$

where G_0 is a Green function:

$$G_0(r,s) = \begin{cases} \frac{s^2r^2}{2} + s - \frac{9s^2}{5} + \frac{s^4}{2} & \text{if} \quad r < s \\ \frac{s^2r^2}{2} + \frac{s^2}{r} - \frac{9s^2}{5} + \frac{s^4}{2} & \text{if} \quad r \geq s \end{cases}. \tag{4.50}$$

Then we set a non-standard inner product

$$\langle A, B\rangle = \sum_{k=1}^{K} A_k B_k (r_j^0)^2. \tag{4.51}$$

Let $\mathbf{e}_1$, $\mathbf{e}_2$,..., $\mathbf{e}_K$ be an orthonormal basis with respect to the inner product (4.51) and

$$\mathbf{e}_1 = \frac{(1,1,...,1)}{\sqrt{\langle (1,1,...,1),(1,1,...,1)\rangle}}. \tag{4.52}$$

The μ_0's are determined from a $K-1$ dimensional eigenvalue problem:

$$\sum_{m=2}^{K} d_m N_{mn} = \mu_0 \tau d_n, \ n = 2,3,...,K. \tag{4.53}$$

The $K-1$ by $K-1$ matrix N is obtained by projecting the K by K matrix M into the $K-1$ dimensional subspace spanned by $\mathbf{e}_2, \mathbf{e}_3, ..., \mathbf{e}_K$:

$$N_{mn} = \langle M\mathbf{e}_m, \mathbf{e}_n\rangle, \quad m,n = 2,3,...,K. \tag{4.54}$$

The inner product in (4.54) is the one defined in (4.51).

These critical eigenvalues turn out to be all positive. This follows as a consequence of Section IVA. That N is positive definite is equivalent to the fact that r_j^0 minimizes J, defined in (4.40). The latter condition is fulfilled when $\gamma > \gamma_{K,e}$. Hence $l = 0$ is a stable mode. To each one of these $k-1$ λ_0's, the corresponding eigenfunction $\phi_0(r)$ is given with the help of the eigenvector $(d_2, d_3, ..., d_K)$ of (4.53):

$$\phi_0(r) = \sum_{j=1}^{K} c_j [H'(\frac{r-r_j}{\epsilon}) + \epsilon P_j'(\frac{r-r_j}{\epsilon})] + O(\epsilon^2), \tag{4.55}$$

where

$$(c_1, c_2, ..., c_K) = \sum_{n=2}^{K} d_n \mathbf{e}_n. \tag{4.56}$$

When l is greater than 0, there are K critical eigenvalue for each l. All of them are of order ϵ^2. If we write

$$\lambda_l = \epsilon^2 \mu_l + O(\epsilon^3), \tag{4.57}$$

then the μ_l's are found by solving the K-dimensional eigenvalue problem

$$[\frac{(l(l+1)-2)\tau}{(r_k^0)^2} + (-1)^k \gamma \mathcal{V}(r_k^0)]c_k + \gamma \sum_{j=1}^{K} G_l(r_k^0, r_j^0) c_j = \mu_l \tau c_k, \ k = 1,2,...,K \tag{4.58}$$

where G_l is another Green function:

$$G_l(r,s) = \begin{cases} (\frac{s^{1-l}}{2l+1} + \frac{(l+1)s^{2+l}}{l(2l+1)})r^l & \text{if} \quad r < s \\ s^{2+l}(\frac{r^{-1-l}}{2l+1} + \frac{(l+1)r^l}{l(2l+1)}) & \text{if} \quad r \geq s \end{cases}. \tag{4.59}$$

These critical eigenvalues are not always positive. There exists a stability threshold $\gamma_{K,s}$ so that when $\gamma_{K,e} < \gamma < \gamma_{K,s}$, all the critical eigenvalues are positive and hence the K-interface solution u is stable, and when $\gamma > \gamma_{K,s}$ at lease one critical eigenvalue is negative and the K-interface solution

a	.5	.525	.55	.575	.6	.625	.65	.675	.7	.725
$\gamma_{2,s}$	1162	1067	1002	956	931	919	924	943	951	939
l	4	3	3	3	3	3	3	3	2	2

a	.75	.775	.8	.825	.85	.875	.9	.925	.95	.975
$\gamma_{2,s}$	952	999	1077	1199	1393	1711	2241	3254	5684	15454
l	2	2	2	2	2	2	2	2	2	2

Table 4: The (leading order) values of $\gamma_{2,s}$ for various a and the corresponding mode l.

u is unstable. To each λ_l the corresponding eigenfunctions are $\phi_l(r)Y_{lm}$, $m = 0, \pm 1, ..., \pm l$. ϕ_l is determined with the help of the eigenvectors c_k in (4.58):

$$\phi_l(r) = \sum_{j=1}^{K} c_j [H'(\frac{r - r_j}{\epsilon}) + \epsilon P_j'(\frac{r - r_j}{\epsilon})] + O(\epsilon^2). \tag{4.60}$$

Table 4 reports the stability threshold values for various a. Note that the $\gamma_{2,s}$'s are greater than the corresponding $\gamma_{2,e}$. Hence there is a range $(\gamma_{2,e}, \gamma_{2,s})$ for γ where the 2-interface spherical lamellar pattern is stable.

5 Discussion

The single sphere pattern studied in Section 3 only gives a limited picture of the spherical phase of a diblock copolymer, where multiple spheres co-exist. Moreover the spheres are observed to pack in the body centered cubic pattern. An analytic study of such a multi-sphere pattern requires more refined singular perturbation techniques. The main difficulty is that the spheres in such a phase are only approximately round. The following argument illustrates this point.

It is known that even in a general domain, which we call Ω, (2.9) has a singular limit as $\epsilon \to 0$ [28]. The leading order outer expansion u^0 of u, a solution of (2.9), has the property that for a.e. $x \in \Omega$ $u^0(x) = 0$ or $u^0(x) = 1$ and $\overline{u^0} = a$. Let S be the union of the interfaces that separate the regions $u^0 = 0$ (B-rich micro-domains) from the regions $u^0 = 1$ (A-rich micro-domains), and $v^0 = (-\Delta)^{-1}(u^0 - a)$. In the singular limit the thickness of the interfaces is 0. Then one requires that at every $x \in S$

$$\tau\kappa(x) + \gamma v^0(x) = \eta^0 \tag{5.61}$$

where $\kappa(x)$ is the mean curvature of S at x viewed from the $u^0 = 1$ side, and η^0 is a Lagrange multiplier to be determined. This is the generalization of (4.37). The constraint (4.37) is replaced by $\overline{u^0} = a$. If the free boundary problem (5.61) admits an isolated stable solution u^0, then near u^0 there exists a local minimizer solution u of (2.9). However (5.61) is still a challenging nonlocal geometric problem. Even though Figure 1 (3) suggest that we look for solutions with multiple spheres, (5.61) implies that for such a solution the curvature of the interface of a sphere is in general not constant (there is the impact of v^0), i.e. the spheres are not exactly round, unless we deal with the one sphere or the spherically lamellar solutions in a ball as in this paper.

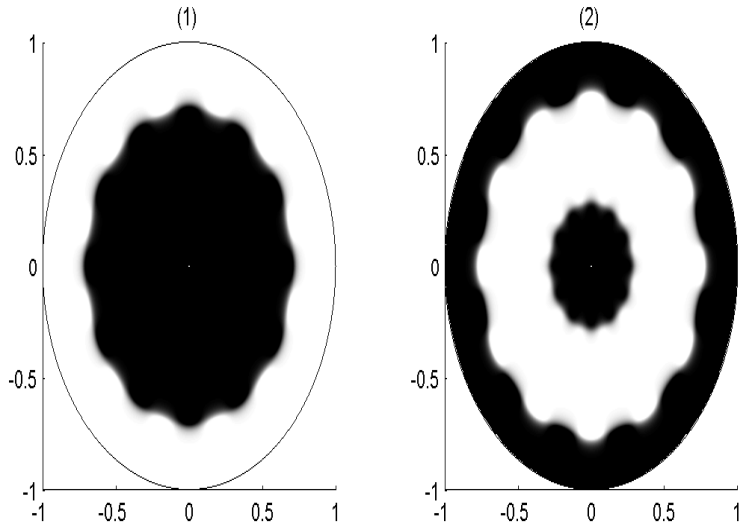

Figure 8: A cross section of a wiggling sphere solution, and a cross section of a wriggled spherical lamellar solution with two interfaces.

Nevertheless if we consider the situation where a is close to 0 (or 1), then v^0 is near constant throughout Ω and hence κ becomes close to a constant and the spheres are approximately round. The spherical phase in Figure 1 is thus heuristically explained.

The stability threshold γ_s (or $\gamma_{K,s}$) is related to a strong segregation bifurcation phenomenon (not to be confused with the bifurcation analysis in the weak segregation regime). When γ passes γ_s (or $\gamma_{K,s}$) a second solution bifurcates out of the sphere (or spherical lamellar) solution. The new solution differs from the old one by a quantity which is roughly proportional to the eigenfunction of the 0 principal eigenvalue at $\gamma = \gamma_s$ (or $\gamma_{K,s}$). Because the eigenfunction has the form (3.29), the new solution has a wiggling interface (or interfaces). The wiggles are determined by the spherical harmonics Y_{lm} in (3.29), Figure 8. Such a wiggling interface solution can be regarded as another defective pattern.

We did not discuss the dynamics of a diblock copolymer system. The purpose of studying the critical eigenvalues of a solution of (2.9) in this paper is to determine whether the solution is a local minimizer of (2.2). However the same critical eigenvalues also determine the local dynamics, near the solution, of the evolution equation

$$u_t = \epsilon^2 \Delta u - f(u) - \epsilon\gamma(-\Delta)^{-1}(u-a) + \overline{f(u)} \tag{5.62}$$

with the boundary condition $\partial_\nu u = 0$ on ∂D. The eigenfunctions of the critical eigenvalues give the directions along which the dynamics of (5.62) runs slowly (the eigenfunctions of the non-critical eigenvalues are directions of fast dynamics).

The critical eigenvalues in this context admit geometric interpretations. For the sphere pattern the eigenfunction of the critical eigenvalue λ_0 in (3.30) is radially symmetric. So the dynamics in this direction involves only the shape change of u in the radial direction. The eigenfunctions of the

critical eigenvalue λ_1 in (3.32) have the forms $(x/r)\phi_1(r)$, $(y/r)\phi_1(r)$ and $(z/r)\phi_1(r)$. They lead to translations of u in x, y, or z directions in the dynamics. Finally the eigenfunctions of the critical eigenvalues λ_l, $l > 1$, in (3.34) give rise to oscillations of the interfaces. The same interpretations are also valid for the spherical lamellar pattern. Because all these eignenfunctions concentrate at the interface r_j by (3.31), (3.33), (4.47), (4.55) and (4.60), the dynamics along the directions of the critical eigenvalues is localized to the motion of the interfaces.

However (5.62) is only one of many dynamical laws one can associate to a diblock copolymer system. A more realistic one is the forth-order partial differential equation [2]

$$u_t = \Delta(-\epsilon^2\Delta + f(u)) - \epsilon\gamma(u - a) \tag{5.63}$$

subject to the boundary conditions $\partial_\nu u = \partial_\nu \Delta u = 0$ on ∂D. (5.63) generalizes the well-known Cahn-Hilliard equation [4]. An even more complex dynamical law considers a diblock copolymer melt as a fluid. It adds the velocity field and couples (5.63) to the Navier-Stokes equation of the velocity field [2].

We are mainly interested in stable solutions of (2.9). However there also exist unstable spherical lamellar solutions even for $\gamma \in (\gamma_{K,e}, \gamma_{K,s})$. In Figures 6 and 7 when $\gamma > \gamma_{2,e}$ in addition to the minimum of J there also exists a local maximum of J. This maximum point corresponds to a unstable spherical lamellar solution. This unstable solution exists for $\gamma \geq \gamma_{2,s}$ as well. The instability of this solution is caused by the $m = 0$ mode.

In the functional (2.2) the key ingredient is the nonlocal term. It describes a long range interaction. Many other important physical systems that exhibit self-organization and pattern formation share the same phenomenon [40]. Examples include charged Langmuir monolayers [1], and smectic liquid crystal films [39]. Many of the singular perturbation techniques presented here may be applied to these problems [27, 32, 35, 34]. In all the examples we find periodic structures that consist of micro-domains delineated by narrow interfaces.

The nonlocal interaction in (2.2) is of Coulomb type [24]. Some of the above mentioned problems have different nonlocal interactions. In the charged monolayer problem the nonlocal term is written as

$$\int_D \int_D (u(x) - a)G_c(x, y)(u(y) - a)\, dxdy \tag{5.64}$$

which assumes the same form as (2.8) does. However the kernel G_c is different. If D is a square, i.e. $(0, 1)^2$, with the periodic boundary condition, then G_c is translation invariant so that $G_c(x, y) = G_c(x - y)$. The Fourier series of G_c is

$$\hat{G}_c(\xi) = \frac{1}{|\xi|}. \tag{5.65}$$

Note that for the diblock copolymer problem the corresponding G on a square is

$$\hat{G}(\xi) = \frac{1}{|\xi|^2}. \tag{5.66}$$

Hence as $|\xi| \to \infty$, (5.66) has a faster decay rate than (5.65) does. Many properties, such as the optimal size discussed in Section IIIB, are sensitive to the decay rates. In general with a slower decay rate, one finds smaller micro-domains [32].

In the smectic liquid crystal film problem, the nonlocal interaction comes from a coupling effect with the director field. In this case, because of the unit length constraint on the director field, the nonlocal interaction is no longer quadratic [34].

References

[1] D. Andelman, F. Broçhard, and J.-F. Joanny. Phase transitions in Langmuir monolayers of polar molecules. *J. Chem. Phys.*, 86(6):3673–3681, 1987.

[2] M. Bahiana and Y. Oono. Cell dynamical system approach to block copolymers. *Phys. Rev. A*, 41(12):6763–6771, 1990.

[3] F. S. Bates and G. H. Fredrickson. Block copolymers - designer soft materials. *Physics Today*, 52(2):32–38, 1999.

[4] J.W. Cahn and J.E. Hilliard. Free energy of a nonuniform system. I. Interfacial free energy. *J. Chem. Phys.*, 28(2):258–267, 1958.

[5] R. Choksi. Scaling laws in microphase separation of diblock copolymers. *J. Nonlinear Sci.*, 11(3):223–236, 2001.

[6] R. Choksi and X. Ren. On the derivation of a density functional theory for microphase separation of diblock copolymers. *J. Statist. Phys.*, 113(1-2):151–176, 2003.

[7] E. De Giorgi. Sulla convergenza di alcune successioni d'integrali del tipo dell'area. *Rend. Mat. (6)*, 8:277–294, 1975.

[8] P. C. Fife and D. Hilhorst. The Nishiura-Ohnishi free boundary problem in the 1D case. *SIAM J. Math. Anal.*, 33(3):589–606, 2001.

[9] I. W. Hamley. *The Physics of Block Copolymers*. Oxford Science Publications, 1998.

[10] E. Helfand. Theory of inhomogeneous polymers: fundamentals of Gaussian random-walk model. *J. Chem. Phys.*, 62(3):999–1005, 1975.

[11] E. Helfand and Y. Tagami. Theory of the interface between immiscible polymers ii. *J. Chem. Phys.*, 56(7):3592–3601, 1972.

[12] E. Helfand and Z. R. Wasserman. Block copolymer theory. 4. narrow interphase approximation. *Macromolecules*, 9(6):879–888, 1976.

[13] E. Helfand and Z. R. Wasserman. Block copolymer theory. 5. spherical domains. *Macromolecules*, 11(5):960–966, 1978.

[14] E. Helfand and Z. R. Wasserman. Block copolymer theory. 6. cylindrical domains. *Macromolecules*, 13(4):994–998, 1980.

[15] M. Henry. Singular limit of a fourth order problem arising in the micro-phase separation of diblock copolymers. *Adv. Differential Equations*, 6(9):1049–1114, 2001.

[16] K. M. Hong and J. Noolandi. Theory of inhomogeneous multicomponent polymer systems. *Macromolecules*, 14(3):727–736, 1981.

[17] K. M. Hong and J. Noolandi. Theory of phase equilibria in systems containing block copolymers. *Macromolecules*, 16(7):1083–1093, 1983.

[18] R. Kohn and P. Sternberg. Local minimisers and singular perturbations. *Proc. Roy. Soc. Edinburgh Sect. A*, 111(1-2):69–84, 1989.

[19] L. Leibler. Theory of microphase separation in block copolymers. *Macromolecules*, 13(6):1602–1617, 1980.

[20] M. W. Matsen and F. S. Bates. Unifying weak- and strong-segregation block copolymer theories. *Macromolecules*, 29(4):1091–1098, 1996.

[21] M. W. Matsen and M. Schick. Stable and unstable phases of a diblock copolymer melt. *Phys. Rev. Letters*, 72(16):2660–2663, 1994.

[22] L. Modica. The gradient theory of phase transitions and the minimal interface criterion. *Arch. Rat. Mech. Anal.*, 98(2):123–142, 1987.

[23] L. Modica and S. Mortola. Un esempio di Γ^--convergenza. *Boll. Un. Mat. Ital. B (5)*, 14(1):285–299, 1977.

[24] C. B. Muratov. Theory of domain patterns in systems with long-range interactions of Coulomb type. *Phys. Rev. E*, 66:066108, 2002.

[25] Y. Nishiura and I. Ohnishi. Some mathematical aspects of the microphase separation in diblock copolymers. *Physica D*, 84:31–39, 1995.

[26] T. Ohta and K. Kawasaki. Equilibrium morphology of block copolymer melts. *Macromolecules*, 19(10):2621–2632, 1986.

[27] X. Ren and L. Truskinovsky. Finite scale microstructures in nonlocal elasticity. In recognition of the sixtieth birthday of Roger L. Fosdick (Blacksburg, VA, 1999). *J. Elasticity*, 59(1-3):319–355, 2000.

[28] X. Ren and J. Wei. On the multiplicity of solutions of two nonlocal variational problems. *SIAM J. Math. Anal.*, 31(4):909–924, 2000.

[29] X. Ren and J. Wei. Concentrically layered energy equilibria of the di-block copolymer problem. *European J. Appl. Math.*, 13(5):479–496, 2002.

[30] X. Ren and J. Wei. On energy minimizers of the di-block copolymer problem. *Interfaces Free Bound.*, 5(2):193–238, 2003.

[31] X. Ren and J. Wei. On the spectra of 3-D lamellar solutions of the diblock copolymer problem. *SIAM J. Math. Anal.*, 35(1):1–32, 2003.

[32] X. Ren and J. Wei. Soliton-stripe patterns in charged Langmuir monolayers. *J. Nonlinear Sci.*, 13(6):603–624, 2003.

[33] X. Ren and J. Wei. Triblock copolymer theory: Ordered ABC lamellar phase. *J. Nonlinear Sci.*, 13(2):175–208, 2003.

[34] X. Ren and J. Wei. Chiral symmetry breaking and the soliton-stripe pattern in Langmuir monolayers and smectic films. *Nonlinearity*, 17(2):617–632, 2004.

[35] X. Ren and J. Wei. The soliton-stripe pattern in the Seul-Andelman membrane. *Physica D*, 188(3-4):277–291, 2004.

[36] X. Ren and J. Wei. Stability of spot and ring solutions of the diblock copolymer equation. *J. Math. Phys.*, in press.

[37] X. Ren and J. Wei. Droplet solutions in the diblock copolymer problem with skewed monomer composition. preprint.

[38] X. Ren and J. Wei. Wriggled lamellar solutions and their stability in the diblock copolymer problem. preprint.

[39] J. V. Selinger, Z.-G. Wang, R. F. Bruinsma, and C. M. Knobler. Chiral symmetry breaking in Langmuir monolayers and smectic films. *Phys. Rev. Lett.*, 70(8):1139–1142, 1993.

[40] M. Seul and D. Andelman. Domain shapes and patterns: The phenomenology of modulated phases. *Science*, 267:476–483, 1995.

[41] Y. Tsori, D. Andelman, and M. Schick. Defects in lamellar diblock copolymers: Chevron- and Ω-shaped boundaries. *Phys. Rev. E*, 61(3):2848–2858, 2000.